Evaluating Overall Thermal Performance of Metal Curtain Walls Using Large-Scale Testing

Hua Ge, Ph.D., P.Eng. **Paul Fazio, Ph.D., P.Eng.**

ABSTRACT

A comprehensive research program was carried out to establish the overall performance of curtain walls including thermal, condensation, energy, and indoor thermal comfort using a holistic approach. The study aimed at evaluating the relative importance of design details in contributing to the overall performance of curtain walls, to provide recommendations on the improvement of product design for manufacturers and to quantify the benefits provided by advanced systems.

The research work included both laboratory testing and simulation analyses. This paper presents the experimental studies. A two-story full-size test specimen (3.8 m by 6.7 m) made up of two types of curtain wall designs was tested under a series of steady-state and periodic winter conditions in a large-scale environmental chamber. The testing carried out included (1) air leakage tests, (2) thermal performance tests, (3) measurement of the local convection film coefficient, and (4) measurement of local draft induced by cold curtain wall surfaces.

The experimental results indicate the effect of design details on the performance of curtain walls. For example, high-performance glazing unit provides 20% higher condensation resistance than standard double IGU, and the advanced frame system with larger thermal breaks provides 30% higher condensation resistance than the regular frame system. To carry out the experimental study effectively, a number of innovative test procedures were developed. The testing provided a valuable set of experimental data that may be used to validate current and future computer simulation programs.

INTRODUCTION

Metal curtain walls are widely used in commercial buildings and offer many advantages. However, their thermal performance is still low due to the fact that metal curtain walls consist of a large portion of glazing, and glass and metal are high heat conductors. In practice, metal curtain walls are referred to as "heat sink" in heating-dominant climates. The relatively low thermal resistance results in low surface temperatures in winter and thus may cause condensation and thermal discomfort problems in addition to high energy consumption. The thermal resistance of metal curtain walls can be improved by using high-performance glazing units; however, the benefits of high-performance glazing units cannot be fully realized when the performance of the frame is still low. High-performance curtain wall systems are available on the market, but they have difficulty in competing with the "mainstream" products due to the higher cost. The quantitative demonstration of the benefits provided by high-performance curtain walls, such as higher energy savings and improved thermal comfort in heating-dominant cold climates, would help promote the application of advanced systems.

Initially, metal curtain walls grew within the metal window industry and the current methodology and standards developed for evaluating window performance are also used for curtain walls. However, metal curtain walls differ from windows in that they have a much larger continuous glazing portion, more complex configuration, and heat flow at the joints. In the standard approach and in practice, the thermal performance of curtain walls is represented by the glazing panel only, and the thermal resistance of the spandrel panel is

Hua Ge is Director of Building Science Center at British Columbia Institute of Technology and was previously with Concordia. **Paul Fazio** is a professor in the Building Envelope Performance Laboratory, Center for Building Studies, Department of Building, Civil, and Environmental Engineering, Concordia University, Montreal, Quebec, Canada.

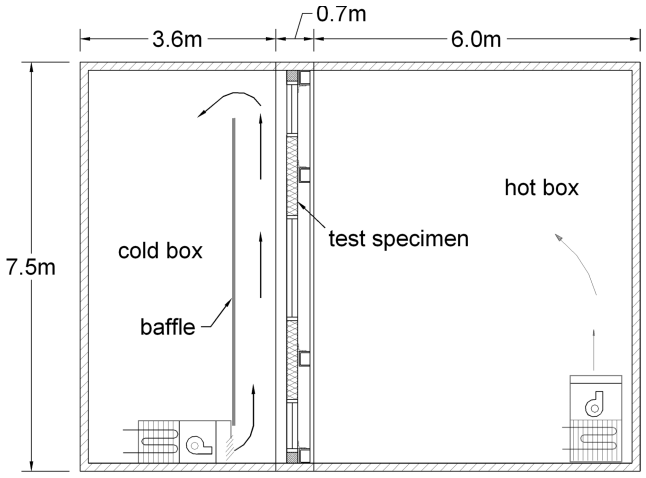

Figure 1 *The experimental setup in the environmental chamber.*

considered by the center area without taking into account the effect of thermal bridges at the window/wall joints. Studies showed that the configuration of frames and thermal bridges, such as steel screws and the return of the back-pan at the joints, significantly reduce the thermal resistance of metal curtain walls (Carpenter and Elmahdy 1994; Ge and Fazio 2002). A simulation using an integrated approach treating curtain walls as integrated systems rather than individual components as prescribed in standards and in practice showed that the existing approach of calculating thermal performance and current practice underestimate the overall thermal transmittance by 20% and the energy consumption by 13% (Ge 2002). Therefore, it is necessary to assess the performance of curtain walls by treating them as systems integrated over larger areas of the envelope than simply the window areas.

A comprehensive study was carried out to evaluate the overall performance of curtain walls including thermal, condensation, energy, and indoor thermal comfort. The research work included both laboratory testing and simulation analyses. This paper presents the experimental study on a two-story curtain wall section carried out in a large-scale environmental chamber. The testing carried out included (1) air leakage tests, (2) thermal performance tests, (3) measurement of the local convection film coefficient, and (4) measurement of local draft induced by cold curtain wall surfaces.

TEST FACILITY AND TEST SPECIMEN

The environmental chamber used (Figure 1) for this study can accommodate wall specimens of up to 4.1 m by 7.2 m, which is equivalent to approximately two commercial stories or three residential stories. The facility consists of a cold box and a hot box, and a structural frame holding the wall specimen is set between these two boxes. Temperature and relative humidity can be controlled to follow design conditions in both boxes. The data acquisition system has 800 channels and can measure temperature, moisture content, relative humidity, heat flux, and other parameters. More information about this facility can be found in Fazio et al. (1997).

The test specimen consists of a standard curtain wall system (referred to as system A) and an advanced curtain wall system (referred to as system B). The main difference between these two systems is the much larger thermal break achieved in system B through the use of a reinforced nylon nose in the frame section compared to the thin strip of flexible PVC used in the standard system A (Figure 2). The other two features used in system B include a revised back pan design as shown in Figure 2b, which shifts the connection of the back-pan to the interior flange of the mullion tube to eliminate the thermal bridge created by the return of the back-pan, and the high-performance insulated glazing units. The high-performance IGU has a low-E coating ($\varepsilon = 0.1$) on the exterior surface of the inner pane, 95%/5% argon/air gas filling, and a thermally broken spacer, whereas the standard IGU used in system A is composed of double 6.4-mm-thick clear glass with a 12.7 mm air gap with a conventional aluminum spacer.

The two curtain wall sections, each 1.9 m by 6.7 m in size, were joined together and anchored on the horizontal structural beams of the specimen frame. The junctions between the specimen perimeter and the inner structural frame surface were sealed with a combination of sealant, tapes, rigid insulation, and plywood, as shown in Figure 2c.

TEST PROCEDURES AND RESULTS

The large-scale testing carried out includes air leakage test, extensive temperature monitoring, air temperature and velocity measurement within the boundary layer along the wall surface, and cold draft measurement. The procedure and results for each individual test are reported in this section.

Air Leakage Test

Airtightness is an important index of curtain wall performance. The fan pressurization method is one of the most effective and direct techniques that has been frequently employed in the estimation of air leakage characteristics of building envelope components in both laboratory and field conditions.

The relatively high airtightness and the large size of the test specimen made it difficult to obtain accurate results using the standard pressurization method in this study. A different "flexible air chamber" pressurization/depressurization setup was developed. An air chamber was formed by attaching a layer of polyethylene film (10 mil) onto the aluminum mullion caps from the exterior side. Depressurization of the flexible chamber was chosen over pressurization based on two considerations: (1) depressurization creates smaller volume between the flexible sheet and the specimen surface and, therefore, will significantly reduce the time required to reach pressure equilibrium and increase the speed of the data collection, and (2) the arrangement reduces the tension required to retain the plastic sheet on the mullion cap surface without tearing or introducing air leakage and, thus, allows higher pressure

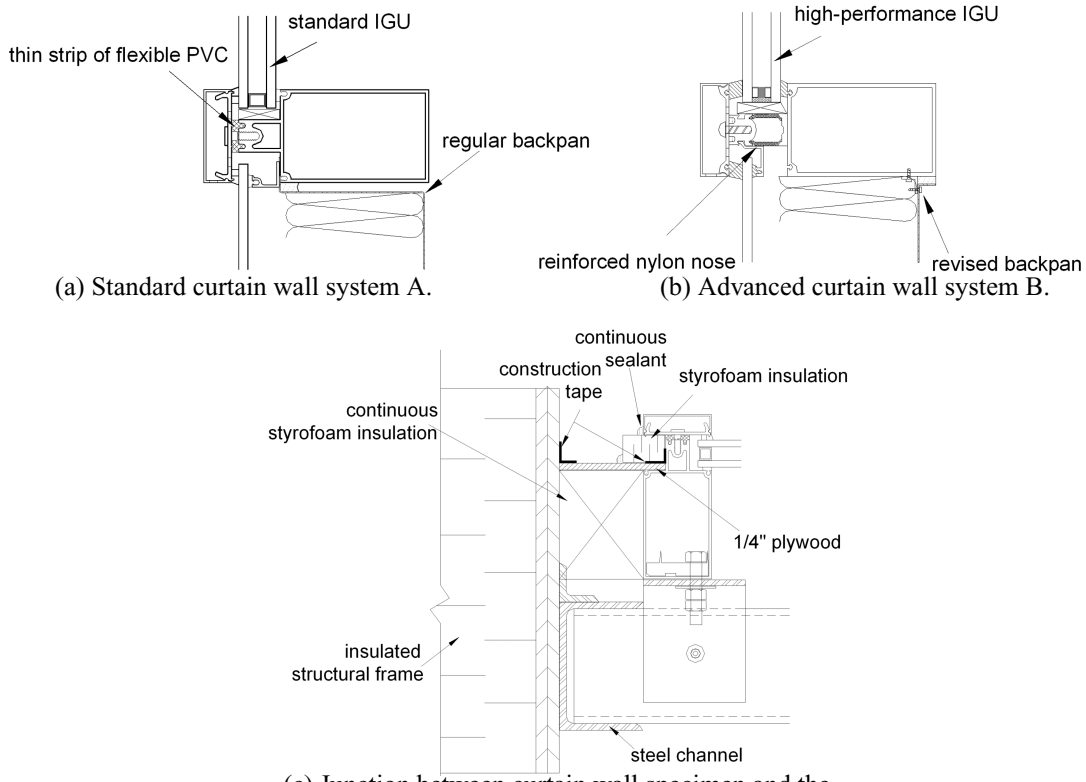

(a) Standard curtain wall system A.

(b) Advanced curtain wall system B.

(c) Junction between curtain wall specimen and the structural frame housing the test specimen.

Figure 2 *Configurations of the test specimen.*

differentials to be achieved. To prevent the contact between the sheets and the wall surface and to provide unhindered air paths to all possible air leakage locations on the surface, metal meshes were placed on the glass pans and small blocks of rigid insulation boards were spaced on the mullion caps (Figure 3).

To calibrate the extraneous air leakage through the inner flexible air chamber, an outer chamber was built to enclose these unintended leakage paths by taping a plastic sheet on the specimen frame that houses the specimen.

The air leakage test was performed individually for each curtain wall section. The air leakage rates under a series of pressure differentials were measured in the single-chamber depressurization setup first and followed by a double-chamber test. Curtain walls are normally required to be tested under 300 Pa due to their wide use in high-rise buildings. Therefore, the pressure difference across the test specimen was built up to as high as 400 Pa in the single-chamber depressurization tests. In the double-chamber depressurization test, the pressure differences between the inner chamber and the outer chamber were maintained at values between 10 and 50 Pa. The pressure differences across the test specimen were maintained from 10 Pa to 300 Pa. The pressure was established first inside the inner chamber, then in the outer chamber. The airflow rate from the inner chamber was measured by a laminar flow element.

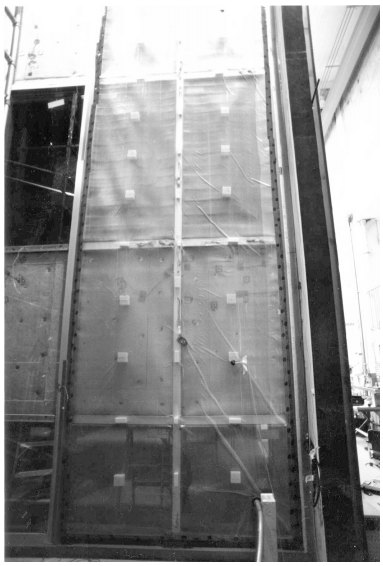

Figure 3 *Test setup for the single-chamber depressurization.*

The air leakage characteristic of each curtain wall section was established by a power law correlation. In the double-chamber test, a sufficient pressure difference must always be maintained across the inner flexible chamber in order to main-

Table 1. Air Leakage Characteristic and Air Leakage Rate Measured for the Curtain Wall Specimen

Curtain Wall	Leakage Characteristics	Air Leakage Rate (L/s) @ 300 Pa	Specimen Area (m^2)	Air Leakage Rate @ 300 Pa (L/s·m^2)
A	$Q = 0.04904(P)^{0.67}$	2.2492	12.78	0.176
B	$Q = 0.07902(P)^{0.65}$	3.2201	12.78	0.252

tain the constant volume of the inner chamber. As a result, the airflows extracted from the inner chamber in the test setup are then composed of air leakage through both the specimen and the extraneous air leakage paths. The air leakage characteristic of the specimen was estimated together with the leakage parameters through the extraneous leakage paths using the least squares regression technique. The details of the analysis can be found in Fazio et al. (2002). Error analyses indicated the reliability of the double-chamber method and its precision. The air leakage characteristics of the curtain walls tested are summarized in Table 1.

Thermal Performance Tests

The thermal performance of curtain walls was evaluated based on the extensive temperature measurements throughout the test specimen. The approach of measuring temperatures was chosen over measuring an average U-factor due to the advantages provided by the detailed temperature measurements: (1) the effect of design details on the thermal performance of curtain walls can be revealed directly by temperature comparisons; (2) condensation resistance can be calculated directly; (3) recorded temperatures can be used to analyze other characteristics, such as the thermal comfort index and the determination of film coefficients; (4) extensive temperature measurements can also be used to validate current and future simulation programs; and (5) detailed temperatures can provide insight on understanding the heat transfer mechanism in curtain walls.

The temperature distribution throughout the test specimen was monitored by approximately 700 type-T (copper-constantan) thermocouples. Thermocouples were installed on the aluminum mullion surfaces, inside mullion channels, and across the mullion sections. Thermocouples were also installed on the glazing surfaces, spandrel back-pan surfaces, and the exterior surface of the 4 in. (101.6 mm) rigid fiberglass insulation in the spandrel panel.

A series of steady-state and periodic winter conditions was simulated in the environmental chamber. These conditions include: (1) outside, $T_o = -5°C$; (2) $T_o = -10°C$; (3) $T_o = -18°C$, CSA winter condition; (4) $T_o = -24°C$, Montreal design condition (99%); (5) $T_o = -32°C$, worst condition (Montreal annual extreme daily mean minimum temperature); (6) $T_o = -12-6\sin(t/12\pi)$ (°C), sinusoidal profile with minimum temperature of –12°C and maximum temperature of –6°C to simulate daily temperature variation (the profile was obtained by analyzing Montreal weather files). The effect of introduced air infiltration on the indoor surface

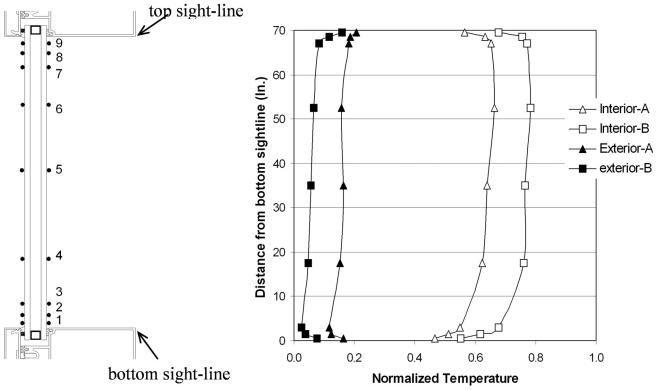

Figure 4 *Normalized temperature profiles along the vertical centerline of glazing panels: the height of the glazing panel is 1.778 m (70 in.),* y *= 0 is at the bottom sight-line, and* y *= 70 is the top sight-line of the glazing panel (the normalization is based on a scale that the outdoor temperature is 0.0 and the indoor temperature is 1.0).*

temperatures and on the condensation resistance was also studied. A 150 Pa pressure differential was introduced across the test specimen by depressurizing the hot box when the CSA winter condition had been maintained for 12 hours. The depressurization lasted for four hours. The temperatures were monitored before, during, and after the depressurization until temperatures returned to the initial values stabilized before the depressurization. The adoption of 150 Pa was based on the field test by Ganguli and Dalgliesh (1988), which found that the pressure differential induced by the stack effect and mechanical systems could be as high as 150 Pa at the 24th floor under a 40°C temperature differential. The indoor temperature was maintained at 21°C and the relative humidity in the hot box was maintained below 25% during all the tests.

The detailed temperature comparisons between curtain wall systems A and B revealed the effect of design details on the thermal performance. For example, the average temperature on the interior surface of the high-performance glazing panel is about 20% higher than that on the standard glazing units, as shown in Figure 4. The curves plotted in Figure 4 are the normalized temperature profiles along the vertical centerline of the glazing panels. The normalization of surface temperature is based on a scale that the outdoor temperature is 0.0 and the indoor temperature is 1.0. This pattern depicts

Table 2. Measured CRF under CSA Test Conditions with and without Introduced Air Leakage

Curtain Wall	CRF without Air Leakage		CRF with Air Leakage	
	CRF_g	CRF_f	CRF_g	CRF_f
A	59	61	57	57
B	72	78	71	75
Note: All numbers are rounded to whole numbers in accordance with the AAMA standard.				

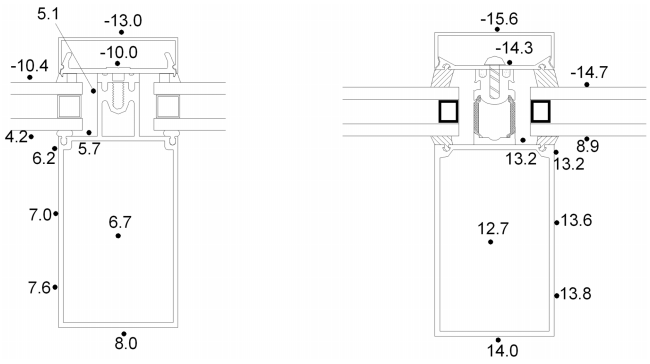

Figure 5 *Selected temperature distribution across the vertical glazing mullions.*

warmer temperatures at the upper part of the glazing and colder at the lower part, with significant temperature variations at the edge-of-glass region and nearly uniform temperatures at the center-of-glass. Surface temperatures under other nontested conditions can be approximated using the normalized temperature index in order to predict the condensation potential for glazing units.

The much larger thermal break used in the frame section of system B results in 6°C higher mullion surface temperature than that of the standard frame system A (Figure 5) under CSA winter conditions. The temperature gradient along the mullion surface in the better insulated system B is smaller than that in system A and more uniform surface temperature is achieved. Similar test results are evident for other steady-state test conditions. The measured thermal response of the specimen to the periodic variation of temperatures also revealed the better thermal performance in system B, indicated by smaller magnitude of temperature variation and longer time lag.

The introduction of air infiltration changes the surface temperatures along and close to the air leakage paths. The temperature response patterns and the variation magnitudes are closely related to the location and the amount of air leakage; therefore, the air leakage characteristics of the specimen are identified by analyzing the transient temperature variation of the extensively monitored locations. Typical air leakage paths identified include:

- Jamb section, which is the connection between the test specimen and the structural frame (Figure 2c). Although taping and sealant were carefully applied at this connection, cracks may have developed under thermal and pressure loads during the tests.
- Steel pins used to hold insulation to spandrel panels. Some of the steel pins were broken or loosened during transportation, leaving a small hole in the back-pan that allowed penetration of cold air. This phenomenon was clearly indicated by the larger magnitude in temperature variation in response to the air leakage in one of the spandrel panels.
- Perimeter of the spandrel panel.

The AAMA procedure (AAMA 1998) was followed to calculate the condensation resistance factor (CRF) for glazing panels with their surrounding frames using measured surface temperatures. In general, without air leakage the high-performance glazing units provide 20% higher condensation resistance than the standard double IGU, and frames with larger thermal breaks provide 30% higher condensation resistance than the standard frame system (Table 2). The introduction of air infiltration has minimal impact on the glazing CRF but considerable impact on the frame CRF. The reduction of glazing CRF is due mainly to the temperature drops at the edge-of-glass. In general, the tested curtain wall itself has good airtightness. The locations where the air leakage has a large effect form along the connection between the curtain wall and the structural frame and along window/wall junctions.

Experimentally Establishing Local Convection Film Coefficients

The indoor/outdoor surface film coefficients are necessary information in evaluating and interpreting the experimental and simulation results. In the standard tests (ASTM 2000) to determine the thermal transmittance through fenestration systems, an average surface film coefficient is normally obtained using the Calibration Transfer Standard. In simulation programs, to calculate the heat transfer through fenestration systems, a simplified constant film coefficient, obtained from correlations developed for free convection over an isothermal plate, is normally assigned for the boundary condition. The use of one constant film coefficient is one of the main reasons for the discrepancy in temperatures between simulation and test results, especially at the edge-of-glass area (Sullivan et al. 1996; Elmahdy 1996; Griffith et al. 1996; de Abreu et al. 1996; Zhao et al. 1996). A different approach was

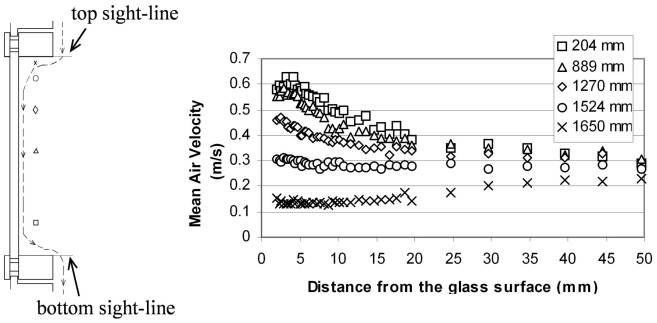

Figure 6 *Selected air velocity profiles in the direction normal to the glass surface at five different distances from the bottom sight-line along the vertical centerline of glazing panel under CSA winter condition (the distance indicated in the figure is from the bottom sight-line).*

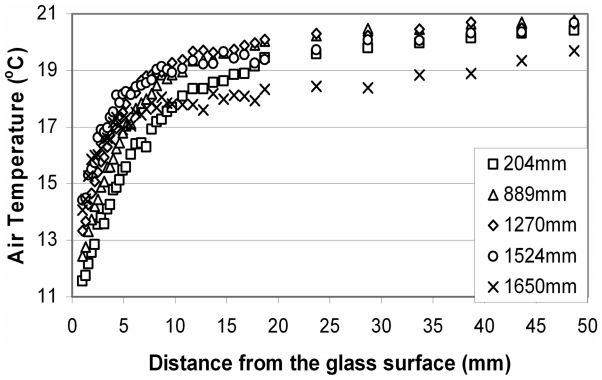

Figure 7 *Selected air temperature profiles in the direction normal to the glass surface at five different distances from the bottom sight-line along the vertical centerline of the glazing panel under CSA winter condition (the distance indicated in the figure is from the bottom sight-line).*

employed in this study to determine the local convection coefficients along the interior glazing surfaces of curtain walls. The experimentally determined local convection film coefficients can be used in simulations to improve the accuracy of programs such as VISION/FRAME (EEL 1995) in predicting the condensation potentials for curtain walls.

The basis of the experimental approach employed is the free natural convection theory presented by Raithby and Hollands (1975). In the boundary layer formed along a cooled vertical plate, the air velocity profile has a local maximum value where the boundary layer can be divided into inner region and outer region. In the inner region, there is no momentum transfer perpendicular to the wall, and pure conductive heat transfer can be reasonably assumed. Therefore, the temperature profile is approximately linear within the inner region and Fourier's equation can be used to calculate the heat flux. The local convection film coefficient can be obtained using the following equations:

$$q_c = k\left(\frac{DT}{Dy}\right) \tag{1}$$

$$h_c = \frac{q_c}{(T_\infty - T_{surf})} \tag{2}$$

where

q_c = heat delivered to the surface by convection (W/m^2);
h_c = convection film coefficient (W/m^2·K);
k = thermal conductivity of still air (W/m^2·K);
T = air temperature (°C);
y = distance from plate (m);
T_∞ = mainstream air temperature (°C); and
T_{surf} = surface temperature (°C).

A customized three-dimensional computer-controlled traverse system was designed and built to carry out air velocity and air temperature measurements within a very close region to the glass surface (as close as 1 mm from the surface). The three-dimensional traverse system can reach a space volume of 4.1 m long, 1.8 m high, and 0.3 m deep near the glass surface and can cover the entire test specimen horizontally and the middle glazing section vertically. A low-velocity omnidirectional anemometer with range of 0.01~1 m/s was used to measure the air velocity. A 30-gauge type-T (copper and constantan) thermocouple was used to measure the air temperature. The details on the experimental setup and test procedure can be found in Ge and Fazio (2003).

The measured air velocity profiles indicate the existence of a maximum air velocity in the region near the glass surface. The temperature profiles indicate good linearity at the regions very close to the glass surface; thus, pure conduction can be reasonably assumed in the inner region. For example, Figure 6 shows the air velocity profiles, and Figure 7 shows the corresponding temperature profiles at selected distances from the bottom sight-line of the glazing panel in system A. When the cold air flows down the glass surface, the air velocity gets greater and the inner boundary gets thicker. The temperature gradient increases slightly with increase of the distance from the bottom sight-line except for the location at 1650 mm since the airflow is in the recirculation region after the head frame.

Figure 8 shows the calculated local convection coefficients along the vertical centerline of the glazing panel in system A under CSA winter conditions. The convection coefficient slightly increases with height, reaching the high value of 3.10 W/m^2·K at approximately 1400 mm from the bottom sightline, and then drops down to 2.38 W/m^2·K at 1650 mm from the bottom sightline where the airflow is in the recirculation region after the head frame. Within the 100 mm of the bottom edge-of-glass area, the convection coefficient drops significantly when the airflow approaches the frame. Similar profiles of air velocity, air temperature, and local convection

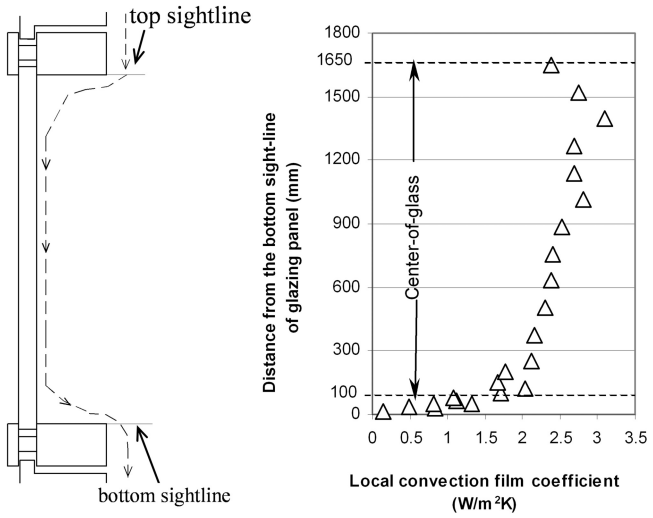

Figure 8 *Local convection film coefficient along the vertical centerline of the glazing panel in system A under CSA winter conditions.*

film coefficient along the vertical centerline were observed for system B.

The local convection film coefficients established using the testing procedure described above were applied in two-dimensional FRAME simulations. The results of the simulations using these film coefficients showed much closer agreement with experimental results in the prediction of condensation performance of the curtain walls (condensation resistance factor of glazing simulated 54 versus 53 tested) than that obtained when using an averaged convection film coefficient (condensation resistance factor of glazing simulated 61 versus 53 tested) (Ge and Fazio 2004a).

Measurement of Cold Draft and Its Impact on Occupants' Thermal Comfort

The large portion of the glazing area in metal curtain walls provides unique architectural effect, natural daylight, and visual contact for occupants with the outdoors. However, in cold winters, the glazing surface may become a cause of discomfort for occupants in the perimeter zone due to the high radiative heat exchange between the human body and the cold glass surface and due to the cold draft induced by air typically flowing off the glazing surface. An experiment was set up in the environmental chamber to study the profile of the cold draft induced by curtain wall surfaces and the effect of this cold draft on the thermal comfort of the occupants.

A simple living space was simulated by adding to the wall specimen, at the spandrel level, a temporary floor on the indoor side. The measurements included two parts: the first part measured the velocity and temperature of the cold air after it flowed off the frame and before it hit the floor; the second part measured the velocity and temperature of the cold draft after it hit the floor and penetrated into the occupied zone. A

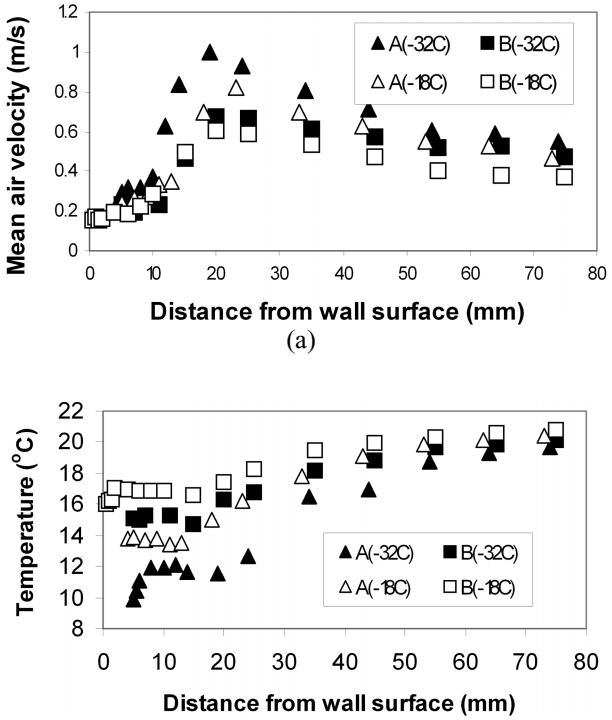

Figure 9 *Horizontal velocity and temperature profiles at 10 mm below the upper edge of frame under CSA test conditions: –18°C and 21°C indoors and Montreal's worst conditions: –32°C outdoors.*

low-velocity omnidirectional anemometer with range of 0.01~1 m/s was used to measure the air velocity, and a 30-gauge type-T (copper and constantan) thermocouple was used to measure the air temperature of the cold draft. Further details on the test setup can be found in Ge and Fazio (2004b).

The measurements along the spandrel panel indicate that the cold draft induced by the high-performance glazing panel is much less than that induced by the standard glazing panel. For example, Figure 9 shows the air velocity and temperature profiles at 10 mm below the upper edge of the frame (below the bottom sight-line) for both wall systems under two test conditions: one with outdoor temperature of –18°C and the other with outdoor temperature of –32°C. The air velocity increases with the increase of the distance from the wall surface until it reaches a maximum value and then it drops. The location of the peak velocity value is the core of the cold draft. The maximum velocity in the cold draft formed in system A is about 40% higher than that in system B (0.82 m/s versus 0.60 m/s) under CSA winter conditions. The temperature increases continuously with the increase of the distance from the wall surface, as shown in Figure 9b, and the temperature in the core of the cold draft is 1.4°C higher in system B than that in system A (17.5°C versus 16.1°C) under CSA winter conditions. When the outdoor temperature was lowered to –32°C, the

Table 3. Mean Air Velocity, Air Temperature, and Percentage of Dissatisfied in the Occupied Zone at 0.1 m above the Floor under CSA Winter Conditions ($T_{outdoor}$ = –18°C and T_{indoor} = 21°C) for Both Curtain Wall Systems

		Distance from Wall Surface (m)			
		0.3	0.6	1.2	2.0
Mean velocity (m/s)	A	0.24	0.23	0.17	0.09
	B	0.19	0.18	0.13	0.06
Temperature (°C)	A	18.4	18.8	19.3	19.9
	B	18.6	18.9	19.3	19.9
PD (%)	A	24.3	24.0	16.6	6.6
	B	19.7	17.7	12.9	3.0

difference in air velocity and air temperature of the cold draft formed along the two curtain wall systems increased. The maximum velocity in the cold draft formed in system A is about 50% higher than that in system B (0.997 m/s versus 0.670 m/s) and the temperature in the core of the cold draft is 4.7°C higher in system B than that in system A (16.2°C versus 11.5°C) under Montreal's worst conditions.

The velocity and temperature of the cold air moving along the floor were measured at ankle level (0.1 m from the floor) and results are listed in Table 3. The thermal sensation due to cold draft was evaluated following ASHRAE procedure (ASHRAE 1992). The velocity of the cold air gradually decreases when it moves along the floor. The mean air velocity measured for system A is about 30% higher than that for system B. The temperature difference in the cold draft formed by the two wall systems is not significant and diminishes when the cold air moves along the floor in the occupied zone. The improved wall system B reduces the percentage of dissatisfied due to local draft by 5% compared to the conventional wall system A. In summary, the better insulated system provides better thermal environment for occupants seated in the perimeter zone indicated by smaller velocity, warmer temperature, and lower percentage of dissatisfied.

CONCLUSION

A series of large-scale tests was carried out on a two-story full-size curtain wall specimen made up of two different curtain wall systems, one traditional (A) and one advanced (B). The specimen also included different types of glazing units. The temperature measurements throughout the test specimen indicated that the high-performance glazing unit provides 20% higher condensation resistance than the standard double IGU, and frame system B with larger thermal breaks provides 30% higher condensation resistance than regular frame system A. The air leakage tests indicated that the curtain wall specimen has good airtightness, and the impact of air leakage on the condensation resistance is minimal for the glazing area and considerable for the frame. The locations where the air leakage has a large effect form along the connection between the curtain wall and the structural frame and along window/wall junctions. The measurement of cold draft showed that the advanced wall system B induces less forceful cold draft and provides better thermal comfort index than the standard system A. The experimental approach presented in this paper yielded reasonable results in establishing local convection film coefficients and the application of these local convection film coefficients in simulations improved the accuracy in predicting the condensation performance for fenestration systems. The experimental data together with simulation analyses established the overall performance of metal curtain walls including thermal performance, condensation performance, indoor thermal comfort, and energy consumption. The holistic approach employed yielded a more accurate and more realistic evaluation on the overall performance of metal curtain walls.

ACKNOWLEDGMENT

The authors express their appreciation to the Natural Sciences and Engineering Research Council (NSERC) of Canada for their financial support and to Kawneer Company Canada Ltd. for providing the design, materials, and installation for the test specimen.

REFERENCES

AAMA. 1998. *Voluntary test method for thermal transmittance and condensation resistance of windows, doors and glazed wall sections*. Standard 1503, American Architectural Manufacturers Association.

ASHRAE. 1992. *ANSI/ASHRAE Standard 55-1992, Thermal Environmental Conditions for Human Occupancy.* Atlanta: American Society of Heating, Refrigerating and Air-Conditioning Engineers, Inc.

ASTM. 2000. *Standard C1199, Standard test method for measuring the steady-state thermal transmittance of fenestration system using hot box methods*. Philadelphia: American Society for Testing and Materials.

Carpenter, S., and A.H. Elmahdy. 1994. Thermal performance of complex fenestration systems. *ASHRAE Transactions* 100(2):1179-1186.

CSA. 1998. *Energy Performance of Windows and Other Fenestration Systems, CAN/CSA A440.2*. Canadian Standard Association.

de Abreu, P.F., R.A. Fraser, H.F. Sullivan, and J.L. Wright, 1996. A study of insulated glazing unit surface temperature profiles using two-dimensional computer simulation. *ASHRAE Transactions* 102(2):497-507.

EEL. 1995. FRAMEplus toolkit, version 4.0. Kitchener, Ontario: Enermodal Engineering Ltd.

Elmahdy, A.H. 1996. Surface temperature measurement of insulating glass units using infrared thermography. *ASHRAE Transactions* 102(2):489-496.

Fazio, P., J.W. Rao, and H. Ge. 2002. Measuring air leakage characteristics with flexible double air chambers. *Journal of Architectural Engineering* 8(3) [September]: 89-95.

Fazio, P., A. Athienitis, C. Marsh, and J. Rao. 1997. Environmental chamber for investigation of building envelope performance. *J. of Architectural Engineering* 3(2):97-102.

Ganguli, U., and W.A. Dalgliesh. 1988. Wind pressures on open rain screen walls: Place Air Canada. *Journal of Structural Engineering* 114(3):642-656.

Ge, H., and P. Fazio. 2004a. Effect of boundary conditions on the prediction of temperature distribution for curtain walls. *ASHRAE Transactions* 110(2).

Ge, H., and P. Fazio. 2004b. Experimental investigation of cold draft induced by two different types of glazing panels in metal curtain walls. *Building and Environment* 39(2) [Feb.]:115-125.

Ge, H., and P. Fazio. 2003. Experimentally establishing local convection film coefficients for a standard metal curtain wall system. *Proceedings of 2nd International Conference on Research in Building Physics, Belgium, Leuven, Sept*, pp. 225-232.

Ge, H., and P. Fazio. 2002. Evaluation of critical factors affecting the thermal performance of metal curtain walls by simulations. *Proceedings of eSim 2002, Montreal*, pp. 112-119.

Ge, H. 2002. Study on overall thermal performance of metal curtain walls. Doctoral dissertation, Concordia University, Montreal, Canada.

Griffith, B.T., D. Türler, and D. Arasteh. 1996. Surface temperature of insulated glazing units: infrared thermography laboratory measurements. *ASHRAE Transactions* 102(2):479-488.

Raithby, G.D., and K.G.T. Hollands. 1975. A general method of obtaining approximate solutions of laminar and turbulent free convection problems. *Advances in Heat Transfer* 11:265-315. Academic Press.

Sullivan, H.F., J.L. Wright, and R. Fraser. 1996. Overview of a project to determine the surface temperatures of insulated glazing units: Thermographic measurement and 2-D simulation. *ASHRAE Transactions* 102(2):516-522.

Zhao, Y., D. Curcija, and W.P. Goss, 1996. Condensation resistance validation project—Detailed computer simulations using finite-element methods. *ASHRAE Transactions* 102(2):508-515.